JOURNAL OF NATURAL PRODUCTS

pubs.acs.org/jnp

Article

Kalparinol, a Salvialane (Isodaucane) Sesquiterpenoid Derived from Native Australian *Dysphania* Species That Suggests a Putative Biogenetic Link to Zerumbone

Yuen Ping Tan, Andrei I. Savchenko, Kylie A. Agnew-Francis, Glen M. Boyle, Paul V. Bernhardt, James A. Fraser, and Craig M. Williams*

Cite This: *J. Nat. Prod.* 2020, 83, 1473−1479

Read Online

ACCESS | Metrics & More | Article Recommendations | Supporting Information

ABSTRACT: *Dysphania* is a genus of plants endemic to the Australian continent, occurring primarily in arid and temperate zones. Despite their prevalence, very little in the way of phytochemical and/or bioactivity investigation of native *Dysphania* has been performed. Herein reported is the isolation and elucidation of (6*E*,9*E*)-zerumbone epoxide and a hitherto unreported isomer, (6*Z*,9*E*)-zerumbone epoxide, from *D. kalpari*. In addition, a novel isodaucane sesquiterepene, kalparinol, was isolated from both *D. kalpari* and *D. rhadinostachya*. The coisolation of the humulene and isodaucane skeletons, combined with the lack of any cadalane systems, could suggest an alternate novel biogenetic pathway originating from zerumbone, which is unlike any other proposals for the isodaucene system.

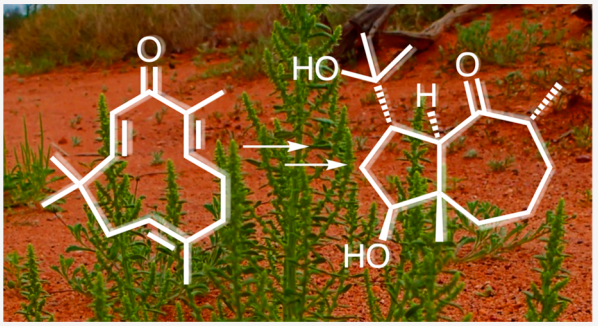

The salvialane[1] (or isodaucane[2,3]) skeleton (**1**) belongs to a rare class of sesquiterpenoids,[4] which to-date have seldom been isolated from plants.[5] The biogenesis of the skeleton has two postulated origins as outlined in Scheme 1. Bohlmann et al.[2] suggested that the isodaucene skeleton (**3**) arises from an acid-induced rearrangement (e.g., via the α-cadinol derivative **4**), which is derived from farnesyl pyrophosphate (**5**), via a sequence involving first rearrangement to nerolidyl diphosphate (**6**) en route to the cadalane skeleton (**7**).[6] Although Bohlmann's postulate has been synthetically substantiated,[7] along with the total synthesis of various isodaucane sesquiterpenes,[8] no experimental evidence surrounding the biogenetic relationship between cadalane and isodaucene currently exists. A separate mechanistic pathway was conceived by König and Bülow,[9] who identified several derivatives of the isodaucane skeleton (e.g., **8**) resulting from acid-catalyzed rearrangements of germacrene D (**9**), an important biogenetic precursor of many other sesquiterpene scaffolds. This finding was later used to provide mechanistic rationale underpinning the presence of unusual sesquiterpenoid chemistry in the Euphorbiaceae family.[10] However, while the germacrene D pathway appears chemically reasonable, it remains uncertain whether or not this macrocyclic intermediate is indeed biogenetically related to isodacane or isodaucene. In the case of the closely related daucene (**2**), radiotracer studies using ^{14}C-labeled sodium acetate eliminated this pathway as contributing to its biosynthesis. Soucek believed the results instead advocated for a pathway involving the cyclization of farnesyl pyrophosphate without a methyl transposition [e.g., via α-cadinol (**10**)].[11]

In continued efforts to survey the phytochemical composition of Australian desert and arid zone flora,[12] we recently detected oxygenated humulenes (e.g., **11**)[13] from two members of the Acacia family, *Dysphania kalpari* and *Dysphania rhadinostachya*, which inspired a re-examination of these plant systems in search of related zerumbone derivatives. Disclosed herein is the isolation of zerumbone (**12**),[14] (6*E*,9*E*)-zerumbone-2,3-epoxide (**13**),[15] (6*Z*,9*E*)-zerumbone-2,3-epoxide (**14**), and kalparinol (**15**), which represents the first isolation of an isodaucane skeleton together with known and novel zerumbone-derived metabolites.

RESULTS AND DISCUSSION

The crude extract from *Dysphania kalpari* was subjected to[1] fractionation (described previously),[13,14] which focused on both the alkene and oxygenated methine ^{1}H NMR spectroscopic region (δ_H 5.0−6.8 and δ_H 2.2−3.2). These fractions were further refined to give pure isolates containing zerumbone (**12**), (6*E*,9*E*)-**13**, and (6*Z*,9*E*)-zerumbone epoxide

Received: October 21, 2019
Published: April 17, 2020

https://dx.doi.org/10.1021/acs.jnatprod.9b01039
J. Nat. Prod. 2020, 83, 1473−1479

Scheme 1. Chemically Substantiated Biosynthetic Considerations by Bohlmann, and Later by König, as Well as Herein Proposed Biosynthesis Surrounding the Isodaucene and Humulene Skeletons

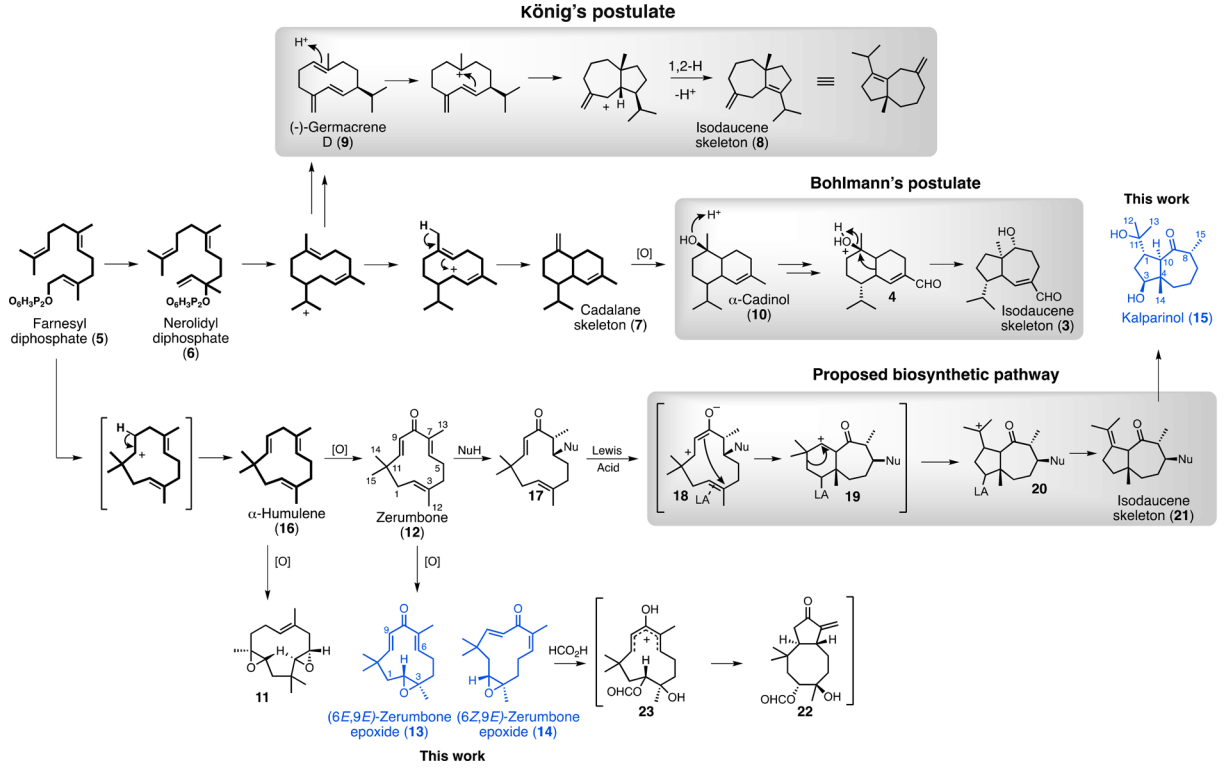

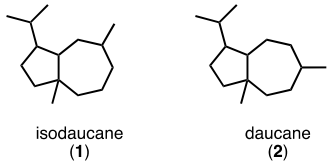

Figure 1. Isodaucane (**1**) and daucane (**2**).

(**14**), as well as kalparinol (**15**), whose structures were elucidated as detailed below. A similar process was utilized for *D. rhadinostachya*, which afforded kalparinol (**15**), but not the zerumbone epoxides (**13** and **14**), although zerumbone (**12**) was detected.

(6*E*,9*E*)-Zerumbone-2,3-epoxide (**13**) was isolated as a colorless solid and, when analyzed using LRESIMS in positive mode, gave a protonated molecular ion at *m*/*z* 235.1 $[M + H]^+$

Table 1. ^{1}H and ^{13}C NMR Assignment for (6*Z*,9*E*)-Zerumbone-2,3-epoxide (14)

	14			Lu *et al.*, 2004[23]			Kalsi *et al.*, 1980[22]	
position	δ_C[a]	δ_H[b]	multiplicity (*J* in Hz)	δ_C[a]	δ_H[b]	multiplicity (*J* in Hz)	δ_H[b]	multiplicity (*J* in Hz)
1a	39.8	1.39	dd (13.5, 11.7)	42.7	1.48	br s		
1b		1.92	dd (13.5, 2.0)		1.95	d (11)		
2	59.0	2.60	dd (11.7, 2.0)	62.9	2.76	d (11)	2.43	dd (11, 2)
3	61.3			61.4				
4a	38.0	2.06	m	38.2	2.30	br s		
4b		1.33	m		1.43	br s		
5a	27.5	2.07	m	24.7	2.45	br s		
5b		2.39	m					
6	133.1	5.66	ddd (12.3, 2.8, 1.5)	147.8	6.14	d (16.5)	5.57	m
7	137.3			139.5				
8	202.0			203.0				
9	128.9	6.08	d (16.2)	128.3	6.09	d (16.5)	6.15	AB dd (16)
10	157.0	6.46	d (16.2)	159.5	6.12	br s	6.15	AB dd (16)
11	36.3			36.0				
12	19.7	1.35	s	15.6	1.22	s	1.33	overlapping s
13	20.9	1.94	dd (2.3, 1.5)	12.1	1.86	s	1.94	br s
14	29.8	1.11	s	29.8	1.09	s	1.15	s
15	24.0	1.28	s	24.0	1.30	s	1.33	overlapping s

[a]Chemical shifts referenced to $CDCl_3$ (δ_C 77.0) at 125 MHz. [b]Chemical shifts referenced to $CDCl_3$ (δ_H 7.26) at 500 MHz.

https://dx.doi.org/10.1021/acs.jnatprod.9b01039
J. Nat. Prod. 2020, 83, 1473−1479

and 257.1 [M + Na]$^+$. The ^{1}H NMR data (Table SI-2) revealed four methyl groups at δ_H 1.86, 1.30, 1.22, and 1.09 and three olefinic protons that overlap at δ_H 6.12. The ^{13}C NMR data (Table SI-2) revealed 15 carbon signals, which included di- and trisubstituted olefinic double-bond resonances, at δ_C 159.4, 147.7, 139.4, and 128.2, two oxygenated carbons at δ_C 62.8 and 61.4, and one carbonyl carbon at δ_C 202.9. The two oxygenated carbons at δ_C 62.8 and 61.4 suggested the presence of an epoxide moiety. After comparison of the ^{1}H and ^{13}C NMR chemical shifts with literature data, the assignment was confirmed as **13**, which has previously been isolated from *Zingiber zerumbet* Smith.[16] In addition, the absolute configuration was confirmed as drawn (Scheme 1), based on comparison of specific rotation data with synthetic material.[17]

(6*Z*,9*E*)-Zerumbone-2,3-epoxide (**14**) was isolated as a white solid with a sodium adduct ion at *m*/*z* 257.1510 [M + Na]$^+$ (−0.7 Δmmu) in positive mode HRESIMS, corresponding to a molecular formula of $C_{15}H_{22}O_2$. This equated to five indices of hydrogen deficiency (IHD). The ^{1}H NMR data (Table 1) indicated four methyl groups at δ_H 1.11, 1.28, 1.35, and 1.93 and three olefinic protons at δ_H 6.46, 5.66, and 6.08. The ^{13}C NMR data (Table 1) exhibited 15 carbon signals, including di- and trisubstituted double-bond resonances at δ_C 128.9, 133.1, 137.3, and 157.0, two oxygenated carbons at δ_C 59.0 and 61.2, and one carbonyl carbon at δ_C 202.0. The two oxygenated carbons at δ_C 59.0 and 61.2 suggested an epoxide moiety, which allowed for the putative identification as a zerumbone epoxide. While this isolate was found to possess remarkable ^{1}H and ^{13}C NMR similarity to that of **13**, there were some notable differences around the double-bond resonances at C-6 and C-7 as well as Me-12 and Me-13 that did not match the reported data of (6*E*,9*E*)-zerumbone epoxide (**13**). This isolate was therefore tentatively identified as a diastereomer of **13**, likely containing a Δ 6(*Z*) double-bond configuration.

Kalsi et al.[18] had purportedly synthesized (6*Z*,9*E*)-zerumbone-2,3-epoxide by treating zerumbone (**12**) with alkaline H_2O_2 and NaOMe. While not all NMR data were disclosed, there were notable differences in the ^{1}H NMR spectrum specifically at H-2, H-9, and H-10. Interestingly, Lu et al.[19] reported the isolation of (6*Z*,9*E*)-zerumbone-2,3-epoxide from *Buddleia lindleyana* Fort. and subsequently named it buddlindeterpene A. However, on closer inspection of the X-ray structure, provided by Lu et al.[19], it was quickly determined that the authors made an erroneous translation of the ORTEP diagram, revealing instead the (6*E*,9*E*)-isomer (**13**) as buddlindeterpene A. Nevertheless, the *E*/*Z* configuration of **14** herein was established through 1D NOE experiments. Correlations were observed between Me-13 and H-6, Me-15 and H-2 and H-9, and Me-14 and H-10 (Figure 2), which suggested a *trans*-epoxide with a (6*Z*,9*E*)-configuration (Figure 2). The (9*E*)-configuration of the double bond was also clear from the J_{H-H} coupling constant (16.2 Hz) for H-9 and H-10, which was reported in the same sesquiterpene class for a (9*E*)-double bond, as well is in compound **13**.[20] Collectively, these data allowed for the unambiguous identification of **14** as (6*Z*,9*E*)-zerumbone-2,3-epoxide, a previously unreported diastereomer of **13**. The absolute configuration of **14** is tentatively assigned as drawn, based on the absolute configuration determined for **13**.

Kalparinol (**15**) was isolated as crystalline needles with a sodium adduct ion located at *m*/*z* 277.1805 [M + Na]$^+$ (+2.5 Δmmu) in positive mode HRESIMS. Based upon the HRESIMS data, a molecular formula of $C_{15}H_{26}O_3$ was established, which equated to three IHD. The ^{1}H NMR data (Table 2) identified the presence of four methyl groups at δ_H 0.65, 1.09, 1.11, and 1.12 and one oxymethine proton at δ_H 3.72. The ^{13}C and DEPT NMR data (Table 2) indicated the presence of 15 carbons, comprising four methyl groups, four sp^3 methylenes, four sp^3 methines, one oxygenated tertiary carbon, one sp^3 quaternary carbon, and one carbonyl carbon at δ_C 215.8 (C-9).

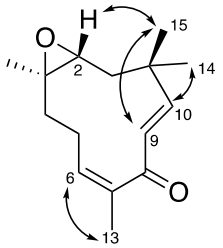

Figure 2. Key NOE correlations for **14**.

Table 2. ^{1}H and ^{13}C NMR Assignments for Kalparinol (15)

position	δ_C[a]	δ_H[b]	multiplicity (*J* in Hz)
1	42.8	2.79	m
2a	32.6	1.88	m
2b		1.69	m
3	82.2	3.72	m
4	46.6		
5a	41.5	1.94	d (10.36)
5b		1.39	d (10.36)
6a	23.6	1.87	m
6b		1.39	m
7a	32.6	1.88	m
7b		1.59	m
8	48.8	2.33	m
9	215.8		
10	55.4	3.03	d (9.10)
11	72.3		
12	26.0	1.12	s
13	29.2	1.09	s
14	13.0	0.65	s
15	20.9	1.11	d (7.31)

[a]Chemical shifts referenced to $CDCl_3$ (δ_C 77.0) at 125 MHz. [b]Chemical shifts referenced to $CDCl_3$ (δ_H 7.26) at 500 MHz.

COSY correlations between H-2 (δ_H 1.88, 1.69, 2H) and H-1 (δ_H 2.79) and H-3 (δ_H 3.72), as well as those between H-1 and H-10 (δ_H 3.03), indicated a C-10−C-1−C-2−C-3 connectivity (Figure 3). A tertiary hydroxy moiety attached

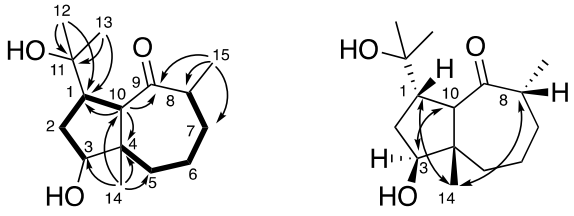

Figure 3. Left: Selected COSY (bold bonds) and HMBC (curved) correlations of kalparinol (**15**). Right: Key NOE correlations.

https://dx.doi.org/10.1021/acs.jnatprod.9b01039
J. Nat. Prod. 2020, 83, 1473−1479

to C-1 was confirmed by HMBC correlations connecting Me-12 and Me-13 to C-1 (δ_C 42.8) and C-11 (δ_C 72.3). Furthermore, HMBC cross-peaks involving H-10 to C-11 (δ_C 72.3), C-1 (δ_C 42.8), and C-4 (δ_C 46.6) and Me-14 to C-3 (δ_C 82.2), C-4, and C-10 indicated the existence of a five-membered ring system (ring A). In addition, the HMBC correlations from Me-14 to C-5 (δ_C 41.5) and H-10 to the carbonyl carbon at C-9 (δ_C 215.8) suggested connectivity to a second ring system (Figure 3).

HMBC cross-peaks arising from connections between Me-15 and C-9 and between C-8 (δ_C 48.8) and C-7 (δ_C 32.6) confirmed connectivity of the second ring from C-9 to C-7 and confirmed the C-8 attachment of Me-15. COSY correlations between H-8, H-7, H-6, H-5, and H-4 thus suggested the second ring to be a seven-membered ring system. NOESY experiments revealed correlations between H-3 and H-10, indicating an α-orientation, and similarly correlations between Me-14 and both H-1 and H-8 confirmed the β-orientation (Figure 3). In addition, an X-ray crystal structure of **15** was obtained, which confirmed the relative configuration and facilitated assignment of the (1*S*, 3*S*, 4*S*, 8*R*, 10*R*) absolute configuration (Figure 4).

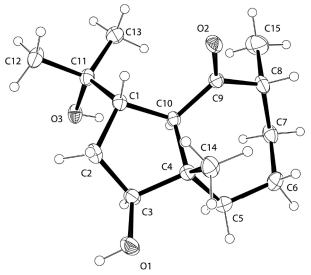

Figure 4. ORTEP view of kalparinol (**15**) with ellipsoids drawn at the 50% probability level.

In terms of the biosynthetic origins of kalparinol (**15**), there is overwhelming synthetic evidence that underpins a third hypothesis originating from zerumbone (**12**). Zerumbone is also biogenetically derived from farnesyl diphosphate (**5**), albeit via the oxidation of α-humulene (**16**) (Scheme 1). Ohe and Uemura,[21] and later John and Radhakrishnan,[22] both demonstrated with various Lewis acids that subsequent to nucleophilic attack (e.g., **17**),[20] which removes the *E*-olefin barrier,[23] the isodaucene skeleton (i.e., **21**) could be accessed via a carbocation-mediated rearrangement from **18**−**20** (Scheme 1). However, when zerumbone epoxide (**13**) was treated with either Brønstead[24] or Lewis acid,[22,25] various transannular cyclization products (e.g., **22**) were observed via a Nazarov intermediate (i.e., **23**),[15,25] but none corresponding to the isodaucene skeleton (Scheme 1). Furthermore, when isodaucane or isodaucene systems have been reported, in the majority of cases they have been coisolated with metabolites containing the cadalane (**7**) or related skeletons,[5] but to-date not with humulene (**16**)-derived metabolites.

Outside of the biogenetic postulates outlined in Scheme 1, a number of other pathways have been suggested based on chemotaxonomic considerations. For example, α-selinane was thought to be a biosynthetic precursor to oxygenated isodaucenes found in *Tritomaria polita* due to the predominance of eudesmane-type structures and high levels of α-selinane in *Tritomaria* species (of the Jungermanniales order).[26] In another report, Chen and Qiu[27] suggested a plausible biogenetic pathway toward novel oxygenated isodaucenes discovered in *Curcuma phaeocaulis* (of the Zingiberales order) via dehydrocurdione, a characteristic constituent of the *Curcuma* genus. This was later reinforced by Kikuchi et al.,[28] who adopted this pathway to rationalize the presence of a novel oxygenated isodaucene from *C. zedoaria*. The observation of isodaucenes from *Curcuma* plants is of particular interest within the context of this work, since these plants are also frequently found to contain zerumbone and zerumbone epoxides.[29]

Based on the synthetic and biogenetic considerations presented above and in Scheme 1, a putative biosynthetic pathway for kalparinol (**15**) is herein proposed as stemming from zerumbone (**12**), but subsequent to reduction of the conjugated $\Delta^{6,7}$ double bond to remove the *E*-olefin barrier (i.e., **24**).[23] Whether epoxidation precedes reduction or not is uncertain. Protonation of the epoxide (i.e., **25**) would induce enolate attack, triggering the transannular cyclization to give the 6,7-bicyclic skeleton as carbocation **26** (Scheme 2). Ring

Scheme 2. Putative Biosynthetic Pathway for Kalparinol (15)

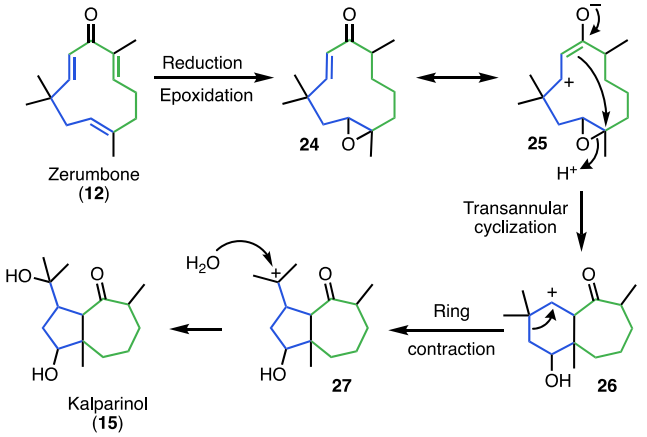

contraction of **26** would give rise to the more stable exocyclic tertiary carbocation **27**, which not only affords the 5,7-bicyclic isodaucane skeleton, but facilitates introduction of the hydroxy group by addition of water (Scheme 2).

Biology. The activity of both zerumbone epoxides was assessed against seven cancer cell lines and one normal human cell line, and five species of pathogenic fungi. Kalparinol (**15**) was not evaluated, as it was observed to be unstable in DMSO solution. The cytotoxicity of (6*E*,9*E*)-**13** and (6*Z*,9*E*)-zerumbone epoxide (**14**) was evaluated against human fibroblast (NFF), melanoma (MM96L), breast cancer (MCF7), hypopharyngeal cancer (FaDu), and four different tongue squamous cell carcinomas (CAL-27, SCC-9, SCC-15, and SCC-25). Results from this evaluation show neither **13** nor **14** to possess any significant cytotoxic activity against the cell lines examined. Antifungal activity of **14** was evaluated through determination of 100% and 50% inhibitory concentration value (MIC and MIC_{50}) against three species of *Candida*, *C. albicans* (ATCC 90028), *C. glabrata* (ATCC 90030), and *C. auris* (CBS 10913 and CBS 12373), as well as *Pichia kudriavzevii* (formerly *Candida krusei*; ATCC 6258). Results from these assays show no activity at ≤200 μM of inhibitor (see Supporting Information, Table SI-1).

https://dx.doi.org/10.1021/acs.jnatprod.9b01039
J. Nat. Prod. 2020, 83, 1473−1479

In conclusion, zerumbone (**12**) and the zerumbone epoxides **13** and **14** were isolated from *D. kalpari*, of which **14** was previously unknown in the literature, although it had been incorrectly described in prior work.[30] In addition, kalparinol (**15**), which contains the rarely occurring isodaucene skeleton, was isolated from both *D. kalpari* and *D. radinostachya*. Given this is the first example of both an isodaucane and humulene skeleton being isolated from the same plant systems, it suggests that an alternative biosynthetic pathway to the isodaucene skeleton is possible as predicted by prior synthetic chemistry investigations.

EXPERIMENTAL SECTION

General Experimental Procedures. Both 1D and 2D ^{1}H NMR spectra were acquired on either a Bruker Avance 500 or 700 MHz spectrometer at 298 K. All ^{13}C NMR spectra were recorded at 125 MHz on a Bruker Avance. Coupling constants are given in hertz (Hz), and chemical shifts are reported as δ values in parts-per-million (ppm), with the solvent resonance as the internal standard (^{1}H NMR ($CDCl_3$) δ 7.26 and ^{13}C NMR ($CDCl_3$) δ 77.0). The optical rotation measurements were carried out by using a JASCO P-2000 spectrophotometer. Infrared spectra (IR) were recorded on a PerkinElmer-400 model, and UV spectra on a PerkinElmer Lambda 35 model. Positive and negative ion electrospray mass spectra (LRESIMS) were measured using a Bruker Esquire HCT or HRESIMS by a MicroTof Q instrument. Purification of fractions via HPLC was carried out using a Shimadzu LC-20AD pump, with an SPD-M20A UV detector and ELSD-LT II light detector. The separation process was conducted using a Phenomenex reversed-phase (RP) C_{18}(2) Luna 10 μm 100 Å column (250 × 10 mm) and a Phenomenex normal-phase (NP) silica Luna 10 μm 100 Å column (250 × 10 mm). TLC was performed using silica gel 60 F254 TLC plates (Merck).

X-ray Crystallography. Data for compound **15** were collected at 190 K on an Oxford Diffraction Gemini CCD diffractometer using Cu Kα radiation (1.541 84 Å). Data reduction was carried out with the CrysalisPro software (Rigaku-Oxford Diffraction). The structure was solved by direct methods and refined with SHELX[31] with all calculations performed with the WINGX package.[32] The thermal ellipsoid plot was created with ORTEP3.[33] The absolute structure was determined by analysis of Friedel pairs using the method of Hooft et al.[34] implemented within PLATON.[35] Data in CIF format have been deposited with the Cambridge Crystallographic Data Centre (CCDC deposition no. 1959347).

Plant Material. *Dysphania kalpari* was collected in August of 2014 from the Cooper Creek basin in Western Queensland, Australia (S 25° 39.360′, E 143° 06.549′). *Dysphania rhadinostachya* was collected in August of 2016 in Welford National Park, Western Queensland, Australia (S 25° 08.801′, E 143° 07.123′). Plant identification was provided with assistance from the Queensland Herbarium, Brisbane.

Extraction and Purification. Whole plant samples were extracted with EtOH (~2 L) at room temperature for approximately six months. The extracts were filtered through a pad of Celite, and the solvent was removed using a rotary evaporator. Subsequently, the crude extract was partitioned between water (200 mL) and EtOAc (3 × 300 mL) to remove salts and water. The EtOAc extract was then concentrated to approximately 50 mL under reduced pressure, washed with brine, and dried over anhydrous Na_2SO_4. Extracts were subsequently dried under high vacuum.

***D. kalpari* Fraction Isolation.** A 942 g sample was extracted as above and concentrated to give 6.1 g of crude extract. This extract was fractionated via flash chromatography on an NP silica gel 60 column (Ø 4.5 × 16 cm). The column was eluted with mixtures of petroleum ether–EtOAc (90:10 (600 mL), 80:20 (400 mL), 70:30 (600 mL), 60:40 (400 mL), 50:50 (400 mL), 40:60 (400 mL), 30:70 (200 mL), 20:80 (200 mL), 10:90 (200 mL), 20:80 (200 mL), 10:90 (200 mL)) and then mixtures of EtOAc–MeOH (100:0 (200 mL), 90:10 (400 mL), 80:20 (400 mL), 70:30 (200 mL), 50:50 (200 mL), and 30:70 (200 mL)). Fractions were pooled into 26 subfractions (E1P21SF1–SF26) based on TLC analysis (i.e., comparing R_f value and color of the bands observed after developing). A 37 mg portion of E1P21SF-7 was purified by semipreparative RP HPLC (MeCN–H_2O, with 80–50% MeCN for 40 min and 2.5 mL/min flow rate; collecting 5 mL/tube) to yield **15** (1.2 mg, t_R 17.7 min). A 43 mg sample of E1P21SF-8 was purified by semipreparative NP HPLC (*n*-hexane–isopropanol, with a 98–90% gradient and 2.5 mL/min flow rate, collecting 5 mL/tube) for 25 min to yield **14** (2.5 mg, t_R 13.9 min). A 25 mg sample of E1P21SF-9 was purified by semipreparative RP HPLC (MeCN–H_2O, with a 60% isocratic run and 3.0 mL/min flow rate; collecting 5 mL/tube) for 35 min to yield **13** (1.5 mg, t_R 27.8 min).

***D. rhadinostachya* Fraction Isolation.** An 834 g sample was extracted as above and extracted to give 6.4 g of crude. This was fractionated using flash chromatography with NP silica 60. A series of solvent gradients was applied containing 90:10 (600 mL), 80:20 (600 mL), 70:30 (600 mL), 60:40 (400 mL), 50:50 (400 mL), 40:60 (400 mL), 30:70 (200 mL), 20:80 (200 mL), 10:90 (200 mL), 20:80 (200 mL), 10:90 (200 mL) petroleum ether–EtOAc and then mixtures of 100:0 (200 mL), 90:10 (400 mL), 80:20 (400 mL), 70:30 (200 mL), 50:50 (200 mL), and 30:70 (200 mL) of EtOAc–MeOH. Fractions were pooled into 26 subfractions (E2P29SF1–SF22) based on TLC analysis. A 28 mg portion of E2P9SF-6 was purified by semi-preparative RP HPLC (MeCN–H_2O, with 50% MeCN and a flow rate of 2.5 mL/min, collecting 5 mL/tube) for 25 min to yield **15** (2.2 mg, t_R 7.2 min).

*(6E,9E)-Zerumbone-2,3-epoxide (**13**):* white powder; $[\alpha]_D^{23}$ +3.5 (*c* 0.15, $CHCl_3$); lit.[36] +2.57; ^{1}H and ^{13}C spectra, see Table S1 and Supporting Information; positive ion LRESIMS *m*/*z* 241.2 $[M + Na]^+$.

*(6Z,9E)-Zerumbone-2,3-epoxide (**14**):* colorless oil; $[\alpha]_D^{23}$ +37.1 (*c* 0.8, $CHCl_3$); ^{1}H and ^{13}C NMR, see Table 1; ^{1}H, ^{13}C, DEPT, HSQC, HMBC, and NOE NMR spectra, see Supporting Information; IR (cm^{-1}) 2959, 2922, 2851, and 1653; UV (MeOH) λ_{max} 231 (1.33) nm; positive ion HRESIMS *m*/*z* 257.1510 $[M + Na]^+$ (calcd for $C_{15}H_{22}O_2Na$–257.1517).

*Kalparinol (**15**):* crystalline needles; $[\alpha]_D^{23}$ −11.5 (*c* 0.10, $CHCl_3$); ^{1}H and ^{13}C NMR, see Table 2 and Supporting Information; IR (cm^{-1}) 3421, 2925, 1693, and 1458.0; UV (MeOH) λ_{max} 207 (0.17) nm; positive ion HRESIMS *m*/*z* 277.1805 $[M + Na]^+$ (calcd for $C_{15}H_{26}O_3Na$ −277.1780); mp 188–192 °C.

ASSOCIATED CONTENT

Supporting Information

The Supporting Information is available free of charge at https://pubs.acs.org/doi/10.1021/acs.jnatprod.9b01039.

Additional information (PDF)

AUTHOR INFORMATION

Corresponding Author

Craig M. Williams − *School of Chemistry and Molecular Biosciences, University of Queensland, Brisbane 4072, Queensland, Australia;* orcid.org/0000-0002-3834-7398; Email: c.williams3@uq.edu.au

Authors

Yuen Ping Tan − *School of Chemistry and Molecular Biosciences, University of Queensland, Brisbane 4072, Queensland, Australia*

Andrei I. Savchenko − *School of Chemistry and Molecular Biosciences, University of Queensland, Brisbane 4072, Queensland, Australia*

Kylie A. Agnew-Francis − *School of Chemistry and Molecular Biosciences, University of Queensland, Brisbane 4072, Queensland, Australia;* orcid.org/0000-0002-7701-9143

Glen M. Boyle − *QIMR Berghofer Medical Research Institute, PO Royal Brisbane Hospital, Brisbane 4029, Queensland, Australia*
Paul V. Bernhardt − *School of Chemistry and Molecular Biosciences, University of Queensland, Brisbane 4072, Queensland, Australia;* orcid.org/0000-0001-6839-1763
James A. Fraser − *School of Chemistry and Molecular Biosciences, University of Queensland, Brisbane 4072, Queensland, Australia*

Complete contact information is available at: https://pubs.acs.org/10.1021/acs.jnatprod.9b01039

Notes

The authors declare no competing financial interest.

■ ACKNOWLEDGMENTS

The authors thank the University of Queensland (UQ) and the QIMR Berghofer Medical Research Institute for financial support. The assistance of Dr. T. Le from UQ for assistance with NMR measurements and Mr. S. Hume from Welford National Park (Queensland Parks & Wildlife Service Department of Environment and Science) is gratefully acknowledged. C.M.W. is grateful to the Australian Research Council for a Future Fellowship award (grant number FT110100851) and for assistance provided by the Queensland Herbarium.

■ REFERENCES

(1) Maurer, B.; Hauser, A. *Helv. Chim. Acta* **1983**, *66*, 2223−2235.
(2) The name isodaucane has been derived from daucane, which is an isomer with the 14-methyl at C-3; see: Misra, L. N.; Jakupovic, J.; Bohlmann, F.; Schmeda-Hirschmann, G. *Tetrahedron* **1985**, *41*, 5353−5356.
(3) (a) For a review on the daucane system, see: Ghisalberti, E. L. *Phytochemistry* **1994**, *37*, 597−623. (b) For biosynthetic considerations of the daucane system, see: Wawrzyn, G. T.; Quin, M. B.; Choudhary, S.; López-Gallego, F.; Schmidt-Dannert, C. *Chem. Biol.* **2012**, *19*, 772−783.
(4) (a) Tchuendem, M. H. K.; Mbah, J. A.; Tsopmo, A.; Ayafor, J. K.; Sterner, O.; Okunjic, C. C.; Iwu, M. M.; Schuster, B. M. *Phytochemistry* **1999**, *52*, 1095−1099. (b) Kikuchi, H.; Sakurai, K.; Oshima, Y. *Org. Lett.* **2014**, *16*, 1916−1919. (c) Fraga, B. M. *Nat. Prod. Rep.* **1987**, *4*, 473−498. (d) Fraga, B. M. *Nat. Prod. Rep.* **2012**, *29*, 1334−1366.
(5) (a) Yoshida, T.; Muraki, S.; Takahashi, K.; Kato, T.; Kabuto, C.; Suzuki, T.; Uyehara, T.; Ohnuma, T. *J. Chem. Soc., Chem. Commun.* **1979**, *11*, 512−513. (b) Yukawa, C.; Iwabuchi, H.; Komemushi, S.; Sawabe, A. *Flavour Fragrance J.* **2005**, *20*, 653−658. (c) Henchiri, H.; Bodo, B.; Deville, A.; Dubost, L.; Zourgui, L.; Raies, A.; Grellier, P.; Mambu, L. *Phytochemistry* **2009**, *70*, 1435−1441. (d) Hu, Y.-M.; Liu, C.; Cheng, K.-W.; Sung, H. H.-Y.; Williams, L. D.; Yang, Z.-L.; Ye, W.-C. *Phytochemistry* **2008**, *69*, 2367−2373. (e) Liu, H.-B.; Zhang, C.-R.; Dong, S.-H.; Yang, S.-P.; Sun, Q.; Geng, M.-Y.; Yue, J.-M. *J. Asian Nat. Prod. Res.* **2012**, *14*, 224−234. (f) Li, X.-S.; Zhou, X.-J.; Zhang, X.-J.; Su, J.; Li, X.-J.; Yan, Y.-M.; Zheng, Y.-T.; Li, Y.; Yang, L.-M.; Cheng, Y.-X. *J. Nat. Prod.* **2011**, *74*, 1521−1525. (g) Appendino, G.; Jakupovic, J.; Jakupovic, S. *Phytochemistry* **1997**, *46*, 1039−1043.
(6) (a) Cordell, G. A. *Chem. Rev.* **1976**, *76*, 425−460. (b) An alternate route to **2** could be derived from the muurolane pathway, see 6a..
(7) (a) Shizuri, Y.; Yamaguchi, S.; Terada, Y.; Yamamura, S. *Tetrahedron Lett.* **1986**, *27*, 57−60. (b) Xia, W. J.; Tu, Y. Q.; Li, D. R. *Synth. Commun.* **2001**, *31*, 1613−1617. (c) Xia, W. J.; Li, D. R.; Shi, L.; Tu, Y. Q. *Tetrahedron: Asymmetry* **2001**, *12*, 1459−1462.
(8) Bülow, N.; König, W. A. *Phytochemistry* **2000**, *55*, 141−168.
(9) (a) Mehta, G.; Krishnamurthy, N.; Karra, S. R. *J. Am. Chem. Soc.* **1991**, *113*, 5765−5775. (b) Harmata, M.; Carter, K. W. *Tetrahedron Lett.* **1997**, *38*, 7985−7988.
(10) García, A.; Delgado, G. *Helv. Chim. Acta* **2006**, *89*, 16−29.
(11) Soucek, M. *Collect. Czech. Chem. Commun.* **1962**, *27*, 2929−2933.
(12) (a) Tan, Y. P.; Savchenko, A. I.; Broit, N.; Boyle, G. M.; Parsons, P. G.; Williams, C. M. *Eur. J. Org. Chem.* **2017**, *2017*, 1498−1501. (b) Tan, Y. P.; Savchenko, A. I.; Broit, N.; Boyle, G. M.; Parsons, P. G.; Williams, C. M. *Fitoterapia* **2018**, *126*, 93−97. (c) Tan, Y. P.; Houston, S. D.; Modhiran, N.; Savchenko, A. I.; Boyle, G. M.; Young, P. R.; Watterson, D.; Williams, C. M. *Chem. - Eur. J.* **2019**, *25*, 5664−5667. (d) Tan, Y. P.; Xue, Y.; Savchenko, A. I.; Houston, S. D.; Modhiran, N.; McMillan, C. L. D.; Boyle, G. M.; Bernhardt, P. V.; Young, P. R.; Watterson, D.; Williams, C. M. *J. Nat. Prod.* **2019**, *82*, 2828−2834.
(13) Tan, Y. P.; Agnew-Francis, K. A.; Hofmann, J.; Savchenko, A. I.; Lafontaine, S. R.; Boyle, G. M.; Bernhardt, P. V.; Fraser, J. A.; Shellhammer, T. H.; Williams, C. M. *Chem. - Eur. J.* **2020**, *26*, 1653−1660.
(14) Rosa, A.; Caprioglio, D.; Isola, R.; Nieddu, M.; Appendino, G.; Falchi, A. M. *Food Funct.* **2019**, *10*, 1629−1642.
(15) Zhang, R.; Feng, X.; Su, G.; Mu, Z.; Zhang, H.; Zhao, Y.; Jiao, S.; Cao, L.; Chen, S.; Tu, P.; Chai, X. *J. Nat. Prod.* **2018**, *81*, 1711−1720.
(16) Ajish, K. R.; Antu, K. A.; Riya, M. P.; Preetharani, M. R.; Raghu, K. G.; Dhanya, B. P.; Radhakrishnan, K. V. *Nat. Prod. Res.* **2015**, *29*, 947−952.
(17) Kitayama, T.; Awata, M.; Kawai, Y.; Tsuji, A.; Yoshida, Y. *Tetrahedron: Asymmetry* **2008**, *19*, 2367−2373.
(18) Kalsi, P. S.; Chhabra, B. R.; Dhillon, R. S.; Wadia, M. S. *Indian J. Chem., Sect. B* **1979**, *19B*, 93−96.
(19) Lu, J.; Tu, G.; Zhao, Y.; Lv, Y.; Liu, L. Y.; Wu, Y. *Magn. Reson. Chem.* **2004**, *42*, 893−897.
(20) Appendino, G.; Minassi, A.; Collado, J. A.; Pollastro, F.; Chianese, G.; Taglialatela-Scafati, O.; Ayyari, M.; Garcia, V.; Muñoz, E. *Eur. J. Org. Chem.* **2015**, *2015*, 3721−3726.
(21) Ohe, K.; Miki, K.; Yanagi, S.-i.; Tanaka, T.; Sawada, S.; Uemura, S. *J. Chem. Soc., Perkin Trans. 1* **2000**, 3627−3634.
(22) Dhanya, B. P.; Gopalan, G.; Sasikumar, P.; Neethu, S.; Meenu, M. T.; Sharathna, P.; John, J.; Varughese, S.; Sabu, M.; Dan, M.; Radhakrishnan, K. V. *Asian J. Org. Chem.* **2018**, *7*, 471−476.
(23) Nishimura, T.; Kawai, J.; Oshima, Y.; Kikuchi, H. *Org. Lett.* **2018**, *20*, 7317−7320; *Org. Lett.* **2019**, *21*, 1241−1241.
(24) Matthes, H. W. D.; Luu, B.; Ourisson, G. *Tetrahedron* **1982**, *38*, 3129−3135.
(25) Minassi, A.; Pollastro, F.; Chianese, G.; Caprioglio, D.; Taglialatela-Scafati, O.; Appendino, G. *Angew. Chem., Int. Ed.* **2017**, *56*, 7935−7938.
(26) Adio, A. M.; Paul, C.; König, W. A.; Muhle, H. *Phytochemistry* **2003**, *64*, 637−644.
(27) Ma, J.-H.; Zhao, F.; Wang, Y.; Liu, Y.; Gao, S.-Y.; Ding, L.-Q.; Chen, L.-X.; Qiu, F. *Org. Biomol. Chem.* **2015**, *13*, 8349−8358.
(28) Kikuchi, H.; Sakurai, K.; Oshima, Y. *Org. Lett.* **2014**, *16*, 1916−1919.
(29) (a) Matthes, H. W. D.; Luu, B.; Ourisson, G. *Phytochemistry* **1980**, *19*, 2643−2650. (b) Zhang, L.; Yang, Z.; Chen, D.; Huang, Z.; Li, Y.; Lan, X.; Su, P.; Pan, W.; Zhou, W.; Zheng, X.; Du, Z. *Chem. Biodiversity* **2017**, *14*, e1700280.
(30) Misassigned structures in the field of natural products is a common occurrence; see for example: Kutateladze, A. G.; Krenske, E. H.; Williams, C. M. *Angew. Chem., Int. Ed.* **2019**, *58*, 7107−7112 and references therein.
(31) Sheldrick, G. M. *Acta Crystallogr., Sect. A: Found. Crystallogr.* **2008**, *64*, 112−122.
(32) Farrugia, L. J. *J. Appl. Crystallogr.* **1999**, *32*, 837−838.
(33) Farrugia, L. J. *J. Appl. Crystallogr.* **1997**, *30*, 565.
(34) Hooft, R. W. W.; Straver, L. H.; Spek, A. L. *J. Appl. Crystallogr.* **2008**, *41*, 96−103.

(35) Spek, A. L. *J. Appl. Crystallogr.* **2003**, *36*, 7−13.
(36) Sadhu, S. K.; Khatun, A.; Ohtsuki, T.; Ishibashi, M. *Nat. Prod. Res.* **2007**, *21*, 1242−1247.

https://dx.doi.org/10.1021/acs.jnatprod.9b01039
J. Nat. Prod. 2020, 83, 1473−1479